

# EXPERIMENTAL STUDY OF ANNULAR TWO-PHASE FLOW ON ROD-BUNDLE GEOMETRY WITH SPACER

Son H. Pham, Zensaku Kawara, Takehiko Yokomine and Tomoaki Kunugi\*

Kyoto University

C3-d2S06, Kyoto-Daigaku Katsura, Nishikyo-Ku, Kyoto, 615-8540 JAPAN

phamhsv@gmail.com; kawara@nucleng.kyoto-u.ac.jp; yokomine@nucleng.kyoto-u.ac.jp;

kunugi@nucleng.kyoto-u.ac.jp

## ABSTRACT

For the rod-bundle geometry of the BWR core, the annular flow consists of wavy liquid films flowing on the fuel rod surfaces and liquid droplets flying in the vapor core between the rods. Although the rod bundle experiments considering liquid droplets have been performed to determine the total their volume, a more detail characteristic such as droplet size has been determined with droplet flow only. In this study, the high speed camera with a back light source has been used to investigate the generation of liquid droplets in annular two-phase flow on a 3x3 simulating BWR fuel rod-bundle with spacers. The experimental arrangement allows the clear visualization of not only the surface of the liquid film flowing on the rod surface but also the liquid droplet flying in the gas core between the rods. The obtained image data show that the droplets are generated through the liquid entrainment phenomena occurring at the liquid film surface, and due to the interaction between the two-phase flow and the spacer. The spacer is seen to introduce a large number of liquid droplets into the gas core and the diameter of some of them can exceed the maximum droplet diameter at upstream, especially at low gas superficial velocities. Furthermore, the quantitative data of droplet diameters are obtained by processing the images. The droplet size distributions at up- and down-streams of the spacer agree well with the qualitative observation. All of the information helps to understand the influences of the spacer on the annular flow.

## KEYWORDS

Annular two-phase flow, Rod bundle, Liquid film flow, Entrainment process, Spacer effects

## 1. INTRODUCTION

The annular two-phase flow exists near the top of the BWR fuel core and keeps an important role in the efficiency as well as the safety of the system. For the rod-bundle geometry of the core, the annular flow consists of wavy liquid films flowing on the fuel rod surfaces and liquid droplets flying in the vapor core between the rods. Despite of this importance, the concerning knowledge is very limited. The main reason is that the distribution of liquid in these two components and the complexities of the rod-bundle geometry including the existence of the spacer have caused many difficulties for the applied experimental techniques.

---

\* Corresponding author

Among the fundamental phenomena of this flow regime which have not been clarified, the generation of liquid droplets strongly affects the momentum, mass and heat transfers in the system. However, the rod-bundle experiments considering liquid droplets have been performed to determine the total their volume [1], while a more detail characteristic such as droplet size has been determined with droplet-flow only [2]. In other words, how the liquid droplets are formed in the annular flow on rod-bundle geometry with spacer has been not clarified.

Based on this point of view, the current study is aimed at providing the visualization data which can describe the mechanisms behind the droplet generation. Firstly, the generation occurring at the liquid film's surface through the liquid entrainment phenomena included in previous work [3] will be recalled. After that, the close-up images taken near a spacer are provided to show how the droplets are generated at this structure. The quantitative data of droplet's size distribution obtained at up- and downstreams of the spacer are also introduced to clarify the influences of this structure starts here with two blank lines before first section title.

## 2. EXPERIMENTAL METHODOLOGY

The detail description of the annular two-phase flow loop was presented in previous paper [3]. The test-section simulating 3x3 BWR fuel rod-bundle consists of a square duct made of transparent acrylic resin and nine steel rod of OD 12 mm which are fixed by three circular ferrule-type spacers as shown in Fig. 1.

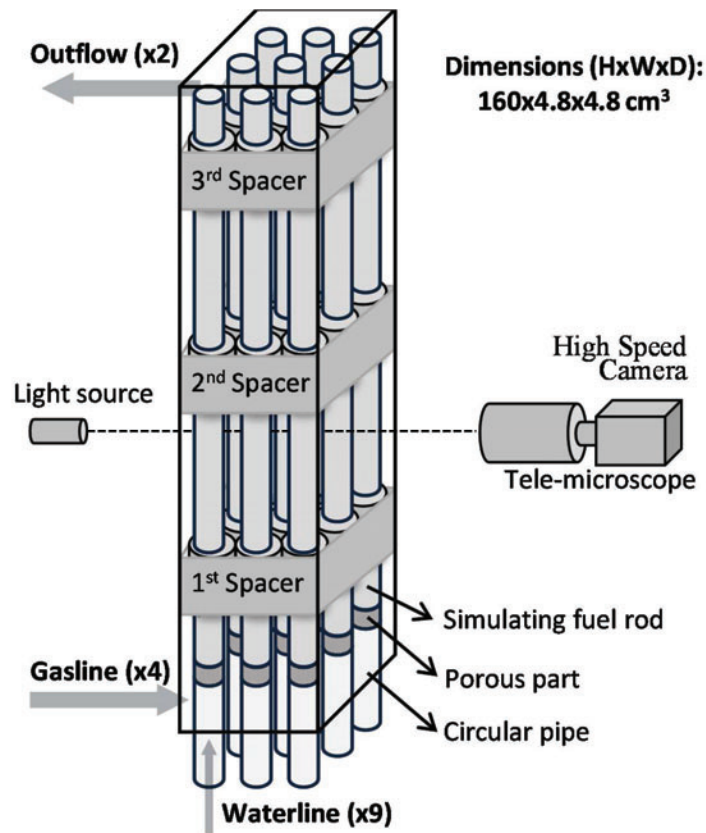
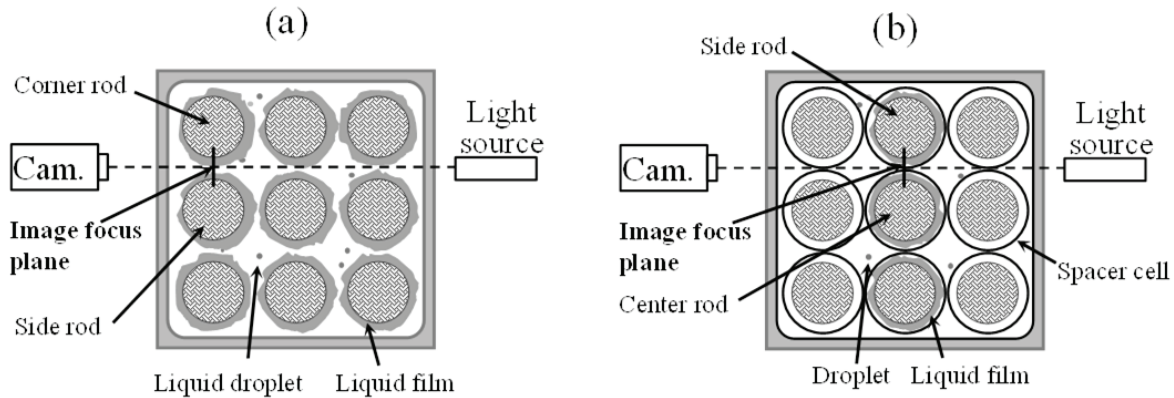


Figure 1 3x3 rod-bundle test-section

The image data are recorded by the system of the high speed camera (Phantom V7.1 - Vision Research Inc.) and the tele-microscope (Cassegrain - Seika Corporation). In the investigation performed at the liquid film surface and the quantitative measurement of droplet diameter, the image focus plane is located at the gap between a corner rod and a side rod as indicated in Fig. 2a. Image distortions caused by the liquid existing on the duct wall is minimized by using an oval-shape obstacle setup on this surface to guide the liquid around the image window. This structure exists locally at the measuring point so its influence on the two-phase flow from the inlet to measuring point and the obtained data is expected to be negligible. The dimension calibration shows that each image pixel represents a physical length of  $\sim 7 \mu\text{m}$  on the image focus plane.



**Figure 2 Optical arrangements: (a) observation at liquid film interface; (b) close-up observation near spacer**

To obtain the size distribution of liquid droplets, the captured image data are processed automatically by using programs developed with Matlab R2012a and its tool boxes. The droplets' boundaries are determined by using the integrated Canny's edge-detection operator [4] which can detect the edges where the sharp changes of intensity occur in the original image. The checking for the measurement of droplet size is performed by using a one-mm transparent spherical particle placed at the image focus plane to simulate the liquid droplet. The diameters obtained by processing the image data agree with the real value within 5%.

Because the spacer itself provides a pathway for the liquid to flow from the rods' surfaces onto the acrylic duct wall, the attempt to avoid the image distortions mentioned above cannot be accomplished for the close-up observation at the spacer. Therefore, six waterlines are turned off and the image focus plane is located at the gap between a side rod and the center rod as indicated in Fig. 2b.

The flow condition used in the investigation of the liquid entrainment phenomena happening at the liquid film surface (previous work) is determined by the gas superficial velocity  $j_G=62.2 \text{ m/s}$  and liquid superficial velocity  $j_L=0.032 \text{ m/s}$ . Meanwhile the quantitative measurement of droplet diameter are performed for the same  $j_L$  and two values of  $j_G=31.8$  and  $62.2 \text{ m/s}$ . The close-up observation near the spacer uses the same water flow rate at each of the three working lines, while the six others are turned off as mentioned above. Therefore, the water superficial velocity in this task is denoted as  $j_{(L \times 3)}$  to hold the same values as before. The gas gage pressure measured near the inlet is about 15.8 and 45.2 kPa for the values of  $j_G$ , respectively. The temperatures of the liquid and the gas flows at this region are maintained about 15 °C and 16 °C, respectively.

It can be seen that the flow conditions with high gas superficial velocity should not be representative to a BWR flow condition. This high gas velocity, however, is necessary to support the clear side-view of the gas-liquid interfaces in current test-section.

### 3. RESULTS AND DISCUSSION

The obtained image data show that the droplets can be generated through the liquid entrainment processes happening at the liquid film surfaces as well as in the interaction between the two-phase flow and the spacer. This section firstly provides the qualitative images of these phenomena. After that, the quantitative data of droplet size distribution obtained at up- and downstreams of the spacer is given to consider the influences of this structure.

#### 3.1. Generation of droplets at liquid film's surface

This part is mainly based on the previous work [3]. As mentioned in the paper, the generation of the liquid droplets could happen at the liquid film through the ligament and bag break-up mechanisms proposed by Azzopardi [5] as illustrated in Fig. 3.

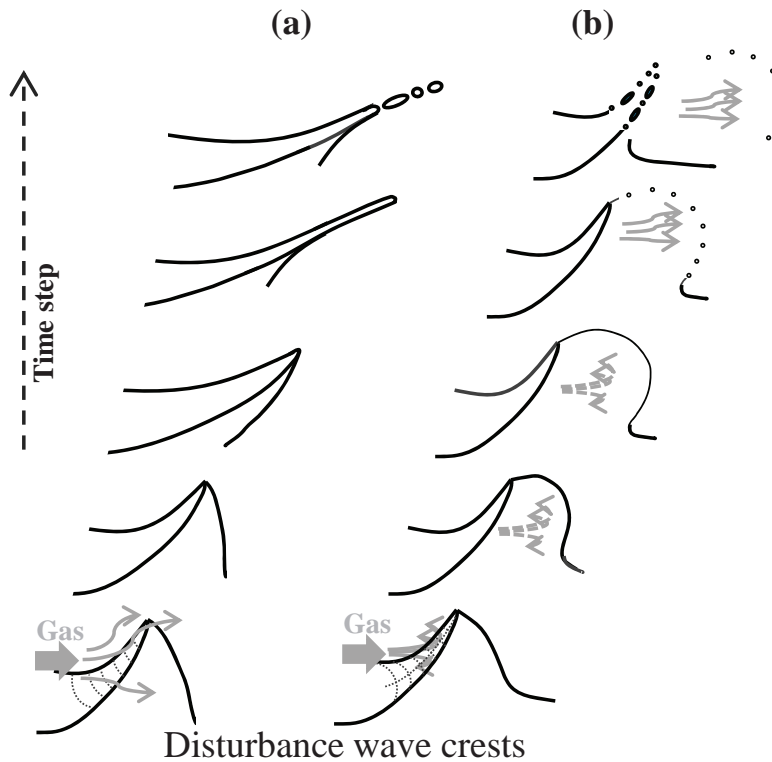


**Figure 3 Liquid entrainment mechanisms: (a) Ligament break-up; (b) Bag break-up**

Figure 4a shows an example of the ligament break-up process in which the wave crest is elongated by the gas flow to form the liquid ligament before it is broken due to the instability to form several droplets. From the obtained image data the ligament is seen to have high possibility to return to the liquid film without the droplet formation. Therefore, the number of droplet generated by the ligament break-up mechanism is quite small but their sizes are as large as the ligament cross-section diameter. The initial

velocities of these droplets are a little bit higher than the wave crest' velocity because the liquid confronted in the ligament already received the momentum from the gas flow during its formation.

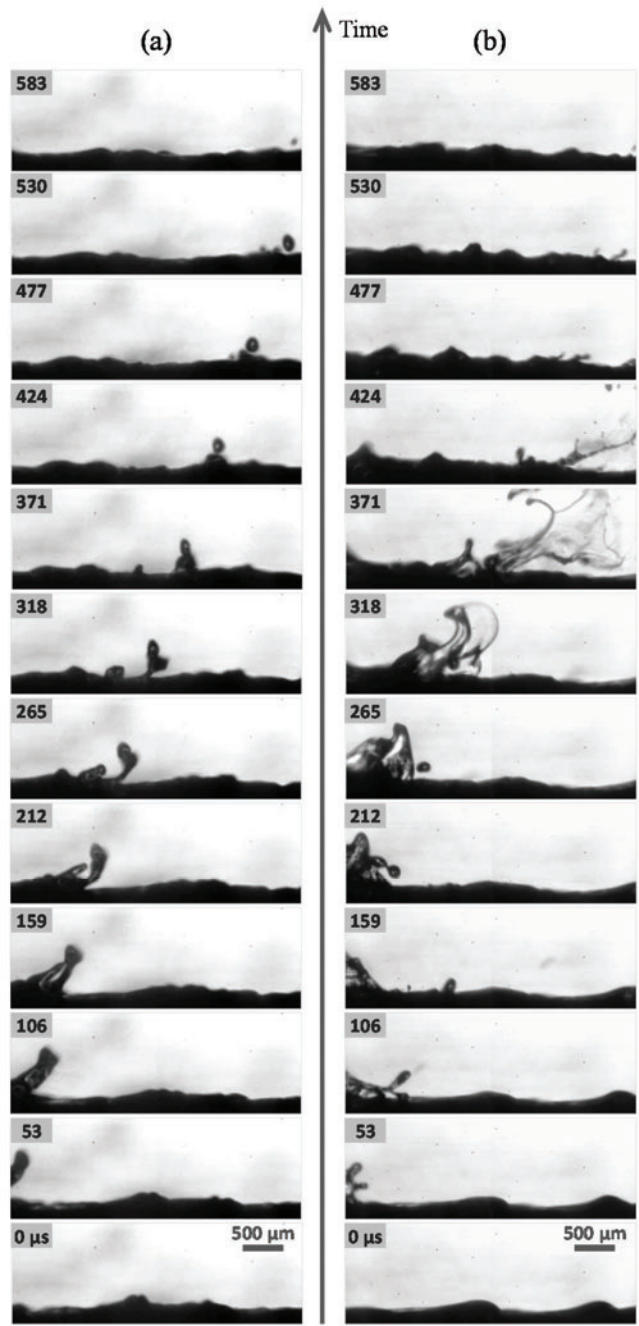


Figure 4 (a) Ligament and (b) bag breakup processes

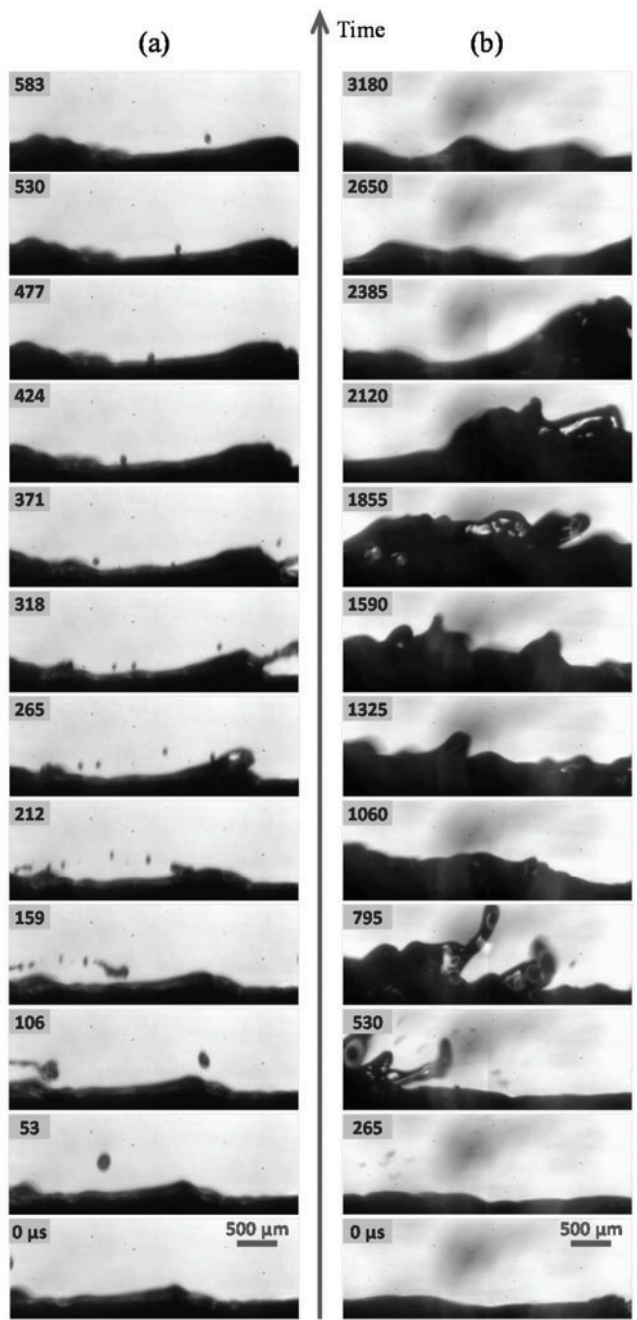


Figure 5 (a) Droplet impingement; (b) Disturbance waves

A bag break-up event is described in Fig. 4b. The gas flow causes an accumulation of the pressure inside the crest to open a bag shape. When the pressure is high enough, the thin layer of this bag is broken into tiny droplets before the breaking of the rim forms some larger droplets. It can be seen that the tiny ones generated at the front part of the bag shape disappear at the next time step because their velocities are high enough to travel away from the image window. These high values of velocity could be reached by the acceleration coming from three sources: (1) the acting force caused by the pressure difference between inside and outside of the bag at the moment of breaking; (2) the surface tension effect occurring

when the instability generated at the thin liquid layer at the front part of the bag at the moment right before the breaking; and (3) the drag force caused by the gas flow. In the other hand, the velocity of the bigger droplets created at the thick rim do not change much after the breaking due to their larger weight and because the breaking of front part of the bag due to the pressure different occurs earlier than the breaking of the rim. Hence, the high pressure inside the bag is already released before the breaking of the rim. However, similar to the ligament break-up case, during the formation of the bag shape, the corresponding amount of liquid already receives some momentum from the gas flow and moves a little bit faster than the main disturbance wave structure.

Besides the liquid entrainment processes caused by the interaction between the gas flow and the liquid film, the impinging of a droplet flying in the gas core on the wave surface can also generate the secondary droplets as shown in Fig. 5a. This mechanism was named as liquid impingement by Ishii and Grolmes [6]. Because these processes can occur at any kind of wave structures, the frequency of occurrence strongly depends on the droplet population and it can be seen from the figure that the amount of entrained liquid caused by this event can be significant.

The authors [3] took the view of Zhao et al. [7] to point out that the disturbance waves consist of the batches of many disturbance crests and they develop on the way from the inlet to regions at further downstream. Therefore, the frequency of ligament and bag break-up processes happening at these disturbance crests is also increased at further downstream. An example of the disturbance waves passing by the image window are given in Fig. 5b.

### 3.2. Generation of droplets caused by spacer

To investigate the generation of droplet at the spacer, the camera system is located at right up- and downstreams of the second spacer, respectively. The vertical angle of the optical system is slightly adjusted to include the spacer cells in the image data. The images captured when all the waterlines are stopped are showed in Fig. 6.

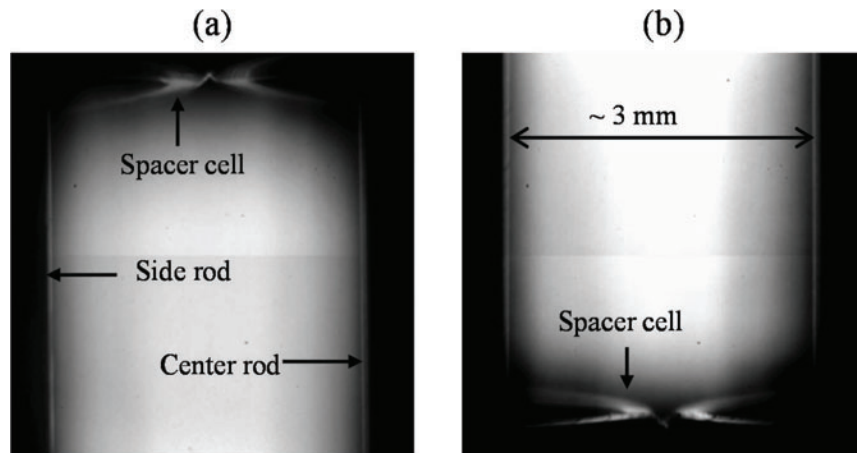


**Figure 6 Images taken (a) right up- and (b) downstreams of the second spacer when all waterlines are turned off**

The situations in which the large-amplitude waves approach the spacer are described by Fig. 7. It can be seen that the wavy films can smoothly enter the spacer region even when there are some wave crests excess the rod-spacer clearance in both case of the gas superficial velocities. Therefore, the interruption of

the spacer hardly causes any separation which can immediately detach an amount of liquid existing in the film put it into the gas core.

Instead, some parts of the liquid will be redistributed on the surface of the spacer cells. When they reach the top of the spacer structure, the generation of droplet occurs as shown in Fig. 8. At lower  $j_G$  (Fig. 8a), the formation of thick ligaments subsequently broken into several large-size droplets are frequently observed.

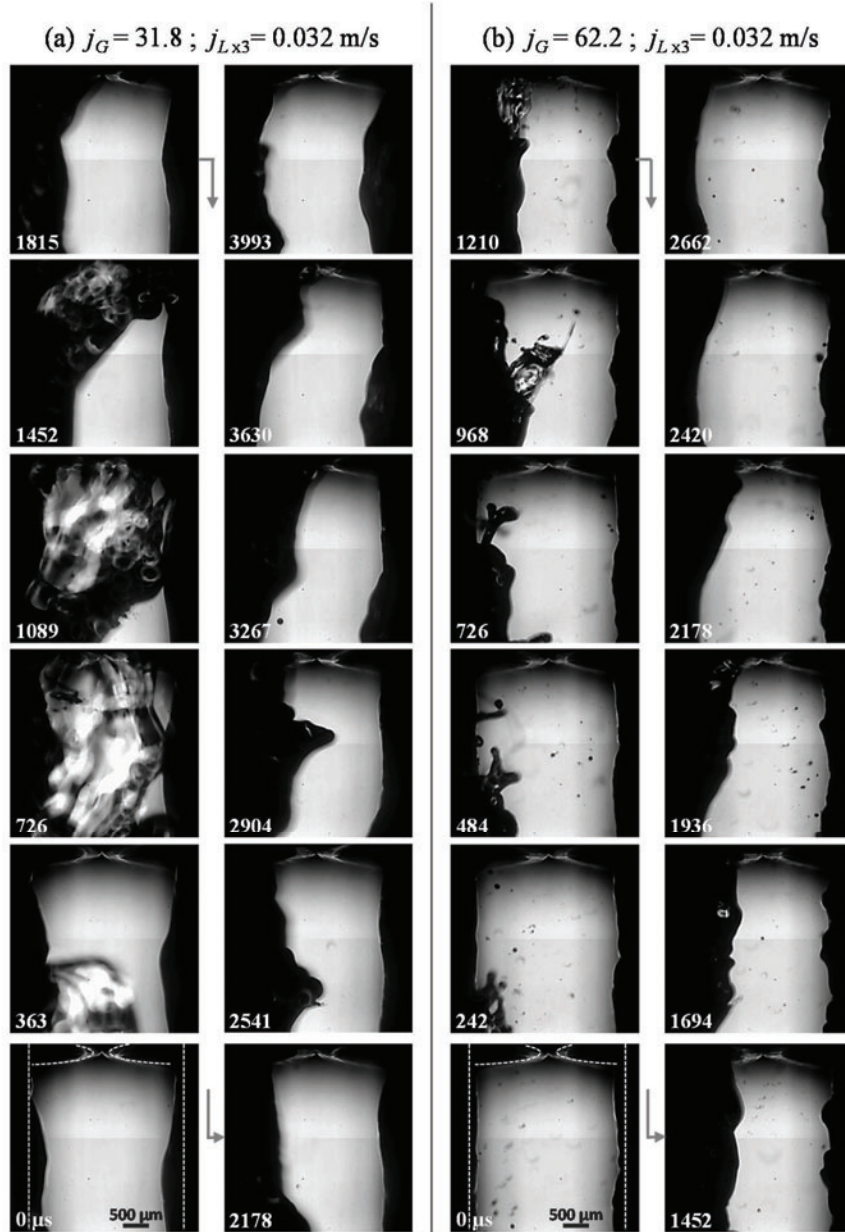


Figure 7 Large-amplitude waves entering spacer

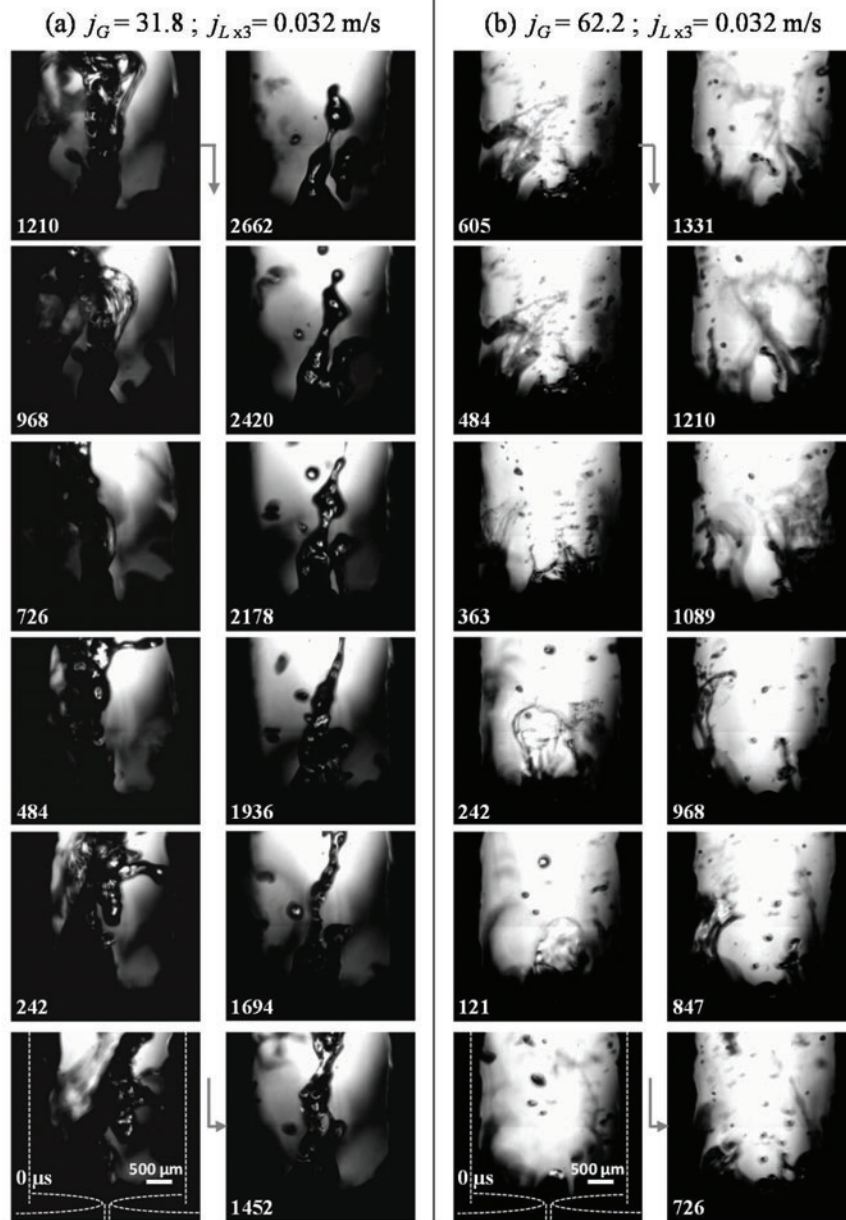
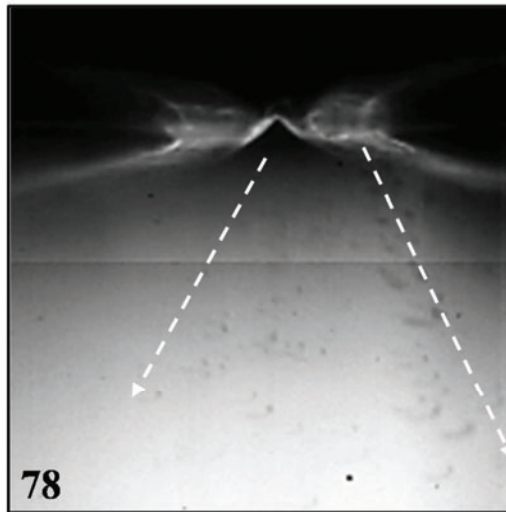


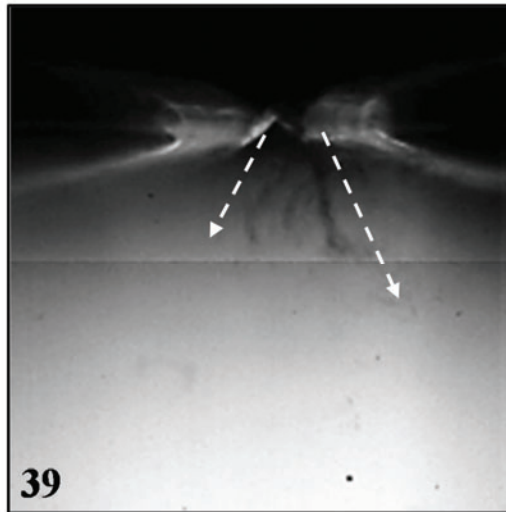
Figure 8 Generation of liquid droplets at top of spacer

In the other hand, Figure 8b corresponding to the high  $j_G$  shows that the generations of droplets mostly happen through the bag break-up mechanism. Similar to the generation at the liquid-film surface, there is a large amount of small-size droplets formed as the bag-shapes are broken. Right after that, the breaking of the rims occurs to form several larger droplets. Because the rims are much thinner than the ligament formed in the low  $j_G$  case, the droplets of the latter group are small compared to the droplets generated with low  $j_G$ .

$$j_G = 31.8$$
$$j_{L \times 3} = 0.032 \text{ m/s}$$



**Bouncing  
back  
secondary-  
droplets**



**Primary  
droplet**

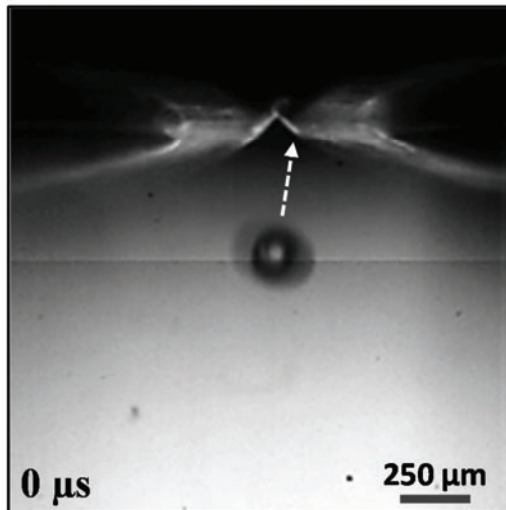


Figure 9 Droplet-spacer interaction

The image data obtained near the spacer also show the typical behaviors of liquid droplets in these regions. Figure 9 describes an impingement of the droplet flying in the gas core on the spacer cell. As the splashing occurs, the primary droplet is broken into many tiny secondary ones. These small-size droplets even bounce back before moving upward with the gas flow and can keep a role in the droplet size distribution obtained at downstream of the spacer.

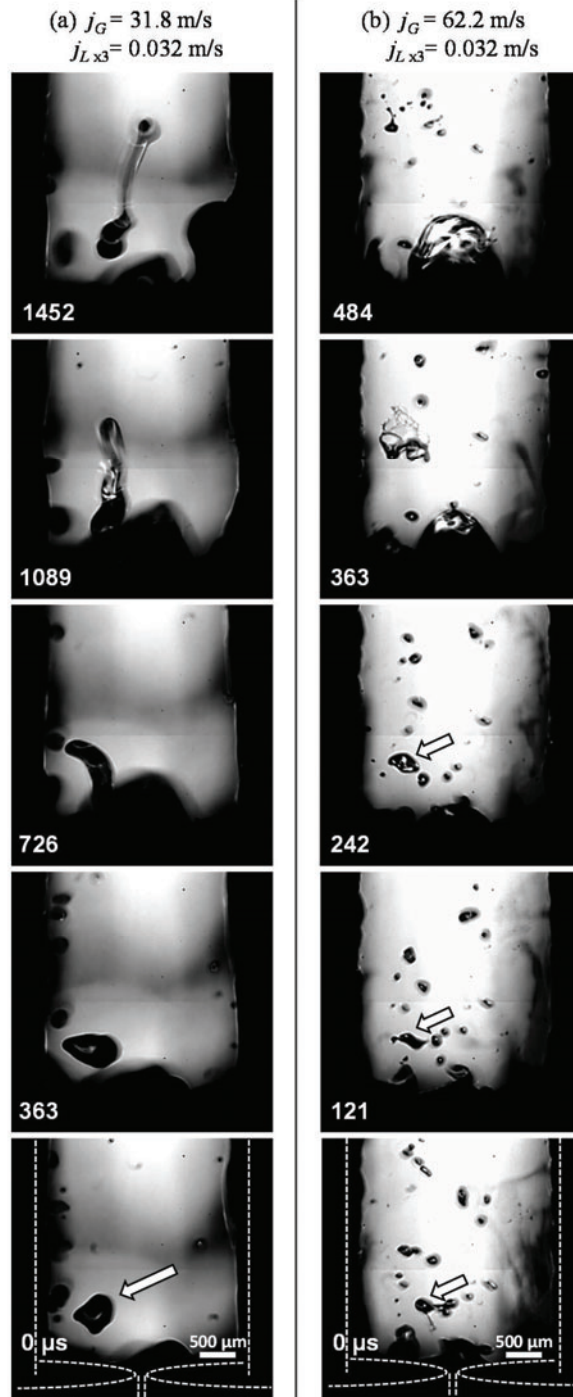


Figure 10 Droplet behaviors at right downstream of spacer

At right downstream of the spacer, a situation commonly observed is when a droplet keeps rotating at the same elevation or falling down despite of the existence of the high gas superficial velocity in the test-section (Fig. 10a and b). The reason for this can be that some flow areas in the spacer region are temporarily blocked due to the formation of liquid bridge. After that, these flow areas are opened again and the exposing of a very low velocity droplet to a local high-velocity gas flow can easily lead to a droplet break-up process. The tiny droplets generated with the bag break-up should also affect the droplet population and size distribution at further downstream of the spacer.

### 3.3. Droplet size distribution

Beside the qualitative visualization, the obtained image data also allow for measurement of the liquid droplets at high time and space resolutions. It should be noticed that the generation of droplet caused by the first spacer is small compared to the second spacer because the first one is located near the inlet where the waves on the liquid film surfaces are in the early stages of development [3, 7].

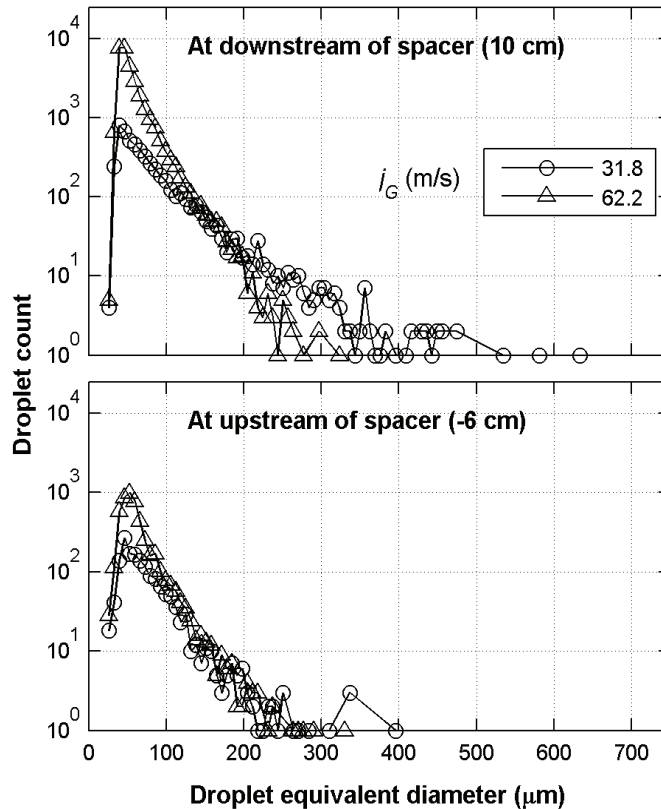


Figure 11 Droplet size distribution

The droplet size distributions captured at 6 cm up- and 10 cm down-streams of the second spacer for both low and high values of  $j_G$  are presented in Fig. 11. These distances are selected to assure that the flow-spacer interaction processes (as seen in Section 3.2) do not appear in the image data and cause difficulties to the image processing. The spacer is seen to introduce a huge number of small droplets into the gas core, especially in the case of high  $j_G$ . Quantitatively the peak height of the droplet size distribution for  $j_G = 62.2$  m/s is increased about ten times through the spacer.

In the case of low  $j_G$ , the data show that the spacer also generates several droplets whose diameters exceed the maximum diameter at upstream. The appearance of these large size droplets can be linked directly to the formation of the thick ligament at the top of the spacer as shown in the Fig. 8a. Meanwhile the generation of small droplets can be considered as the result of the droplet impingement on the spacer cell and/or the breaking of droplets at right downstream of the spacer mentioned above. On the other hand, there is no increase of maximum droplet diameter through the spacer in the case of high  $j_G$ . This point can be approved by the Fig. 8b in which the most liquid distributed on the spacer cells quickly leave this structure in the means of bag break-up processes.

#### 4. CONCLUSIONS

The obtained image data have clarified the mechanisms behind the liquid droplet generation in the annular two-phase flow on rod bundle geometry as follows:

- The liquid entrainment phenomena including bag and ligament break-up processes, and droplet impingement are responsible for the generation of droplets at the liquid film surfaces.
- The flow-spacer interaction introduces a large number of liquid droplets into the gas core. The generation of droplets at the lower  $j_G$  is mostly preceded by a formation of a thick ligament, while the bag break-up processes dominate the droplet generation at higher  $j_G$ .
- These observed differences are reflected in the quantitative data of droplet size distribution. In the lower  $j_G$  case, the spacer generates several large droplets whose diameters exceed the maximum diameters of droplet at upstream of the spacer.

These points would contribute in the development of the physical mechanism-based models for the liquid entrainment phenomena happening in the annular two-phase flow on the rod-bundle with spacers. However, the current experimental arrangement can visualize and measure the liquid droplets at the gap between the corner rod and side rod only. In other words, the data of droplets existing at further inside the test-section or an average variable for whole flow area is not available at the present stage.

In the next steps of this study, the image data will be used to determine the spatial and velocity distribution of the droplets, as well as the thickness and wavy characteristics of the liquid films. These detail information would help to achieve a detail understanding of the influences caused by the spacer on the annular two-phase flow.

#### REFERENCES

1. W. Kraemer, G. Proebstle, W. Uebelhack, T. Keheley, K. Tsuda, S. Kato, "The ULTRAFLOW spacer - an advanced feature of ATRIUM fuel assemblies for boiling water reactors," *Nucl. Eng. Des.* **154**, 17–21 (1995).
2. H.K. Cho, K.Y. Choi, S. Cho, C.-H. Song, "Experimental observation of the droplet size change across a wet grid spacer in a 6×6 rod bundle," *Nucl. Eng. Des.* **241**, 4649–4656 (2011)
3. S.H. Pham, Z. Kawara, T. Yokomine, T. Kunugi, "Detailed observations of wavy interface behaviors of annular two-phase flow on rod bundle geometry," *Int. J. Multiph. Flow* **59**, 135–144 (2014).
4. J. Canny, "A computational approach to edge detection," *IEEE Trans. Pattern Anal. Mach. Intell.* **8**, 679–98 (1986).
5. B.J. Azzopardi, "Mechanisms of Entrainment in Annular Two Phase Flow," *UKAEA Rep. AERE-R 11068* (1983).

6. M. Ishii, M.A. Grolmes, "Inception Criteria for Droplet Entrainment In Two-Phase Concurrent Film Flow," *AIChE J.* **21**, 308–318 (1975).
7. Y. Zhao, C.N. Markides, O.K. Matar, G.F. Hewitt, "Disturbance wave development in two-phase gas-liquid upwards vertical annular flow," *Int. J. Multiph. Flow* **55**, 111–129 (2013).